Passive immunization

Groups of mice were injected twice weekly through the intraperitoneal route with 2 mg (unless otherwise stated) ICSM 18, ICSM 35, IgG1 isotype control (BRIC 222 recognizing CD44; ref. 27) or IgG2b isotype control (BRIC 126 recognizing CD47; ref. 28) antibodies in PBS. Animals were monitored daily for clinical symptoms of scrapie[29] and weighed weekly from 17 weeks after i.c. inoculation or 22 weeks after i.p. inoculation. Clinical signs in untreated mice were first observed approximately 4 weeks before terminal illness (day of death) and included coat ruffling/discoloration, progressive weight loss, bradykinesia (slow movement), tail rigidity, dystonia (clasp foot), kyphosis (hunched back), ataxia and stupor. Weights of scrapie-infected (untreated) mice decreased before terminal illness from 3 and 4 weeks in i.c.- and i.p.-inoculated mice, respectively (Supplementary Fig. 1). Confirmation of scrapie disease was performed by western blot analysis of PrP^{Sc} in brain tissue and in some cases by standard PrP immunohistochemistry.

Immunoprecipitation

Immunoprecipitation of PrP from murine brain tissues using ICSM and BRIC antibodies was performed as described[11].

Western-blot analysis

Spleens were homogenized in PBS to 10% w/v and PrP^{Sc} was precipitated from 500 µl of homogenates using sodium phosphotungstic acid (NaPTA) as previously described[30]. PrP^{Sc} pellets were resuspended in 20 µl of 2% sarkosyl buffer, treated with proteinase K (50 µg ml^{-1}, 50 min, 37 °C), boiled in sample buffer (5 min) and 15 µl aliquots (equivalent to about 2 mg spleen homogenate) were electrophoresed through 16% SDS–polyacrylamide electrophoresis gels. Brain homogenates were diluted to 1% (w/v) in PBS, treated with proteinase K (50 µg ml^{-1} for 60 min, 37 °C) and electrophoresed as for spleens. Proteins were transferred to polyvinylidene fluoride (PVDF) membrane by semi-dry blotting, blocked with TBST/5% non-fat milk, incubated with biotinylated ICSM 18 (0.1 µg ml^{-1}) and developed by enhanced chemiluminescence (Amersham). Semi-quantification was performed by densitometric analysis using MacBas version 2.5 software. At least three to four mice were examined from each treatment group. Bars on graphs are standard deviations. To standardize the PrP^{Sc} signal between blots, 10 µl of PrP^{Sc} precipitated from pooled spleens of terminal (Ter) scrapie-affected mice was loaded on each gel. Densitometric measurement of PrP^{Sc} from treated and untreated spleens was compared to the standard PrP^{Sc} sample and adjusted to relative intensities.

Histology and immunohistochemistry

For PrP^{Sc} immunohistochemistry, spleens and brains were fixed in 10% formalin. Prion infectivity was inactivated by immersion in 98% formic acid and postfixed in formalin for 24 h. Tissues were dehydrated in graded alcohols and xylene, embedded in paraffin, sections cut at 3 µm nominal thickness and stained with haematoxylin and eosin. After antigen retrieval by microwave treatment for 15 min, sections were immunostained with biotinylated ICSM 18 or ICSM 35 on a Ventana automated staining apparatus.

Received 20 September 2002; accepted 27 January 2003; doi:10.1038/nature01457.

1. Collinge, J., Sidle, K. C., Meads, J., Ironside, J. & Hill, A. F. Molecular analysis of prion strain variation and the aetiology of 'new variant' CJD. *Nature* **383,** 685–690 (1996).
2. Bruce, M. E. *et al.* Transmissions to mice indicate that 'new variant' CJD is caused by the BSE agent. *Nature* **389,** 498–501 (1997).
3. Hill, A. F. *et al.* The same prion strain causes vCJD and BSE. *Nature* **389,** 448–450 (1997).
4. Will, R. G. *et al.* A new variant of Creutzfeldt-Jakob disease in the UK. *Lancet* **347,** 921–925 (1996).
5. Prusiner, S. B. Prions. *Proc. Natl Acad. Sci. USA* **95,** 13363–13383 (1998).
6. Enari, M., Flechsig, E. & Weissmann, C. Scrapie prion protein accumulation by scrapie-infected neuroblastoma cells abrogated by exposure to a prion protein antibody. *Proc. Natl. Acad. Sci. USA* **98,** 9295–9299 (2001).
7. Peretz, D. *et al.* Antibodies inhibit prion propagation and clear cell cultures of prion infectivity. *Nature* **412,** 739–743 (2001).
8. Jackson, G. S. *et al.* Reversible conversion of monomeric human prion protein between native and fibrilogenic conformations. *Science* **283,** 1935–1937 (1999).
9. Jackson, G. S. *et al.* Multiple folding pathways for heterologously expressed human prion protein. *Biochim. Biophys. Acta* **1431,** 1–13 (1999).
10. Bueler, H. *et al.* Normal development and behaviour of mice lacking the neuronal cell-surface PrP protein. *Nature* **356,** 577–582 (1992).
11. Beringue, V. *et al.* Regional heterogeneity of cellular prion protein isoforms in the brain. *Brain* (submitted).
12. Beringue, V. *et al.* Opposite effects of dextran sulfate 500, the polyene antibiotic MS-8209, and Congo red on accumulation of the protease-resistant isoform of PrP in the spleens of mice inoculated intraperitoneally with the scrapie agent. *J. Virol.* **74,** 5432–5440 (2000).
13. Souan, L. *et al.* Modulation of proteinase-K resistant prion protein by prion peptide immunisation. *Eur. J. Immunol.* **31,** 2338–2346 (2001).
14. Heppner, F. L. *et al.* Prevention of scrapie pathogenesis by transgenic expression of anti-prion protein antibodies. *Science* **294,** 178–182 (2001).
15. Westaway, D. & Carlson, G. A. Mammalian prion proteins: enigma, variation and vaccination. *Trends Biochem. Sci.* **27,** 301–307 (2002).
16. Klein, M. A. *et al.* PrP expression in B lymphocytes is not required for prion neuroinvasion. *Nature Med.* **4,** 1429–1433 (1998).
17. Montrasio, F. *et al.* Impaired prion replication in spleens of mice lacking functional follicular dendritic cells. *Science* **288,** 1257–1259 (2000).
18. Brown, K. L. *et al.* Scrapie replication in lymphoid tissues depends on prion protein-expressing follicular dendritic cells. *Nature Med.* **5,** 1308–1312 (1999).
19. McKenzie, D., Kaczkowski, J., Marsh, R. & Aiken, J. Amphotericin B delays both scrapie agent replication and PrP-res accumulation early in infection. *J. Virol.* **68,** 7534–7536 (1994).
20. Ingrosso, L., Ladogana, A. & Pocchiari, M. Congo red prolongs the incubation period in scrapie-infected hamsters. *J. Virol.* **69,** 506–508 (1995).
21. Farquhar, C., Dickinson, A. & Bruce, M. Prophylactic potential of pentosan polysulphate in transmissible spongiform encephalopathies. *Lancet* **353,** 117 (1999).
22. Brown, P. Drug therapy in human and experimental transmissible spongiform encephalopathy. *Neurology* **58,** 1720–1725 (2002).
23. Sethi, S., Lipford, G., Wagner, H. & Kretzschmar, H. Postexposure prophylaxis against prion disease with a stimulator of innate immunity. *Lancet* **360,** 229–230 (2002).
24. Sigurdsson, E. M. *et al.* Immunisation delays the onset of prion disease in mice. *Am. J. Pathol.* **161,** 13–17 (2002).
25. Bard, F. *et al.* Peripherally administered antibodies against amyloid β-peptide enter the central nervous system and reduce pathology in a mouse model of Alzheimer disease. *Nature Med.* **6,** 916–919 (2000).
26. Brandner, S. *et al.* Normal host prion protein necessary for scrapie-induced neurotoxicity. *Nature* **379,** 339–343 (1996).
27. Anstee, D. J. *et al.* New monoclonal antibodies in CD44 and CD58: their use to quantify CD44 and CD58 on normal human erythrocytes and to compare the distribution of CD44 and CD58 in human tissues. *Immunology* **74,** 197–205 (1991).
28. Avent, N. D. *et al.* Protein-sequence studies on Rh-related polypeptides suggest the presence of at least two groups of proteins which associate in the human red-cell membrane. *Biochem. J.* **256,** 1043–1046 (1988).
29. Dickinson, A. G., Meikle, V. M. & Fraser, H. Identification of a gene which controls the incubation period of some strains of scrapie agent in mice. *J. Comp. Pathol.* **78,** 293–299 (1968).
30. Wadsworth, J. D. *et al.* Tissue distribution of protease resistant prion protein in variant Creutzfeldt-Jakob disease using a highly sensitive immunoblotting assay. *Lancet* **358,** 171–180 (2001).

Supplementary Information accompanies the paper on *Nature*'s website (http://www.nature.com/nature).

Acknowledgements This work is supported by grants from the Medical Research Council (UK). We thank D. Walsh and S. Gentleman for help with the immunohistochemistry.

Competing interests statement The authors declare competing financial interests: details accompany the paper on *Nature*'s website (http://www.nature.com/nature).

Correspondence and requests for materials should be addressed to S.H. (e-mail: s.hawke@imperial.ac.uk).

Apolipoprotein L-I is the trypanosome lytic factor of human serum

Luc Vanhamme*†, Françoise Paturiaux-Hanocq*†, Philippe Poelvoorde*†, Derek P. Nolan*‡, Laurence Lins§, Jan Van Den Abbeele‖, Annette Pays*, Patricia Tebabi*, Huang Van Xong¶, Alain Jacquet#, Nicole Moguilevsky#, Marc Dieu☆, John P. Kane, Patrick De Baetselier¶, Robert Brasseur§ & Etienne Pays***

** Laboratory of Molecular Parasitology, IBMM, University of Brussels, 12, rue des Profs Jeener et Brachet, B6041 Gosselies, Belgium*
§ Centre de Biophysique Moléculaire Numérique, University of Gembloux, B5030 Belgium
‖ Department of Parasitology, Institute for Tropical Medicine, Antwerp, B2000 Belgium
¶ Laboratory of Cellular Immunology, Free University of Brussels, Sint Genesius Rode, B1640 Belgium
 # Laboratory of Applied Genetics, IBMM, University of Brussels, B6041 Belgium
☆ Unit of Cellular Biochemistry & Biology, University of Namur, B5000 Belgium
*** Cardiovascular Research Institute, University of California, San Francisco, California, 94143-0130 USA*
† These authors contributed equally to this work

Human sleeping sickness in east Africa is caused by the parasite *Trypanosoma brucei rhodesiense*. The basis of this pathology is the resistance of these parasites to lysis by normal human serum (NHS)[1,2]. Resistance to NHS is conferred by a gene that encodes a truncated form of the variant surface glycoprotein termed serum resistance associated protein (SRA)[3,4]. We show that SRA is a lysosomal protein, and that the amino-terminal α-helix of SRA is

‡ Present address: Department of Biochemistry, Trinity College, Dublin 2, Ireland.

responsible for resistance to NHS. This domain interacts strongly with a carboxy-terminal α-helix of the human-specific serum protein apolipoprotein L-I (apoL-I). Depleting NHS of apoL-I, by incubation with SRA or anti-apoL-I, led to the complete loss of trypanolytic activity. Addition of native or recombinant apoL-I either to apoL-I-depleted NHS or to fetal calf serum induced lysis of NHS-sensitive, but not NHS-resistant, trypanosomes. Confocal microscopy demonstrated that apoL-I is taken up through the endocytic pathway into the lysosome. We propose that apoL-I is the trypanosome lytic factor of NHS, and that SRA confers resistance to lysis by interaction with apoL-I in the lysosome.

Trypanosoma brucei brucei infects a wide range of mammals but is unable to infect humans because this *T. brucei* subspecies is lysed by NHS[1,2]. In contrast, *T. b. rhodesiense* exhibits sensitivity or resistance to NHS, depending on antigenic variation. The latter phenotype arises because the gene encoding resistance, *SRA*, is present in just one of the multiple polycistronic units where the genes for the variant surface glycoprotein (VSG) are transcribed[4]. The product of *SRA* is an atypical VSG of shorter than average length (410 amino acids instead of approximately 490)[3]. Anti-SRA antibodies detected a protein with a relative molecular mass of around 50,000 (M_r, 50K; Fig. 1, lanes 1, 2), which accumulates in the lysosome as revealed with a specific marker for the endocytic compartment (tomato lectin, which stains the flagellar pocket, endosomes and lysosome)[5], and antibodies against the lysosomal membrane glycoprotein p67 (ref. 6; Fig. 2a, b).

Because transfection of *SRA* allows *T. b. brucei* to grow in NHS[4] (Fig. 1, lanes 3–5), we investigated the minimal requirements of SRA necessary for resistance by generating trypanosomes expressing various *SRA* mutants (Fig. 3d). These cells were analysed for *SRA* expression and sensitivity to NHS (Fig. 1; see also Supplementary Information). Although SRA contains *N*-linked high mannans (Supplementary Information), these were not involved in resistance, as individual or collective replacement of the putative N-glycosylation sites did not affect SRA-mediated resistance (Fig. 1, lanes 6, 7). The C terminus and glycosyl phosphatidylinositol (GPI) anchoring signal were also dispensable, as truncated SRA versions lacking this region still conferred resistance (Fig. 1, lanes 8, 9). Similarly, deletions of the N-terminal signal peptide or of the most hydrophobic region (amino acids 98–118) were without effect (Fig. 1, lanes 10, 11). Regions between residues 32–97 and/or 119–192 were mapped to be the minimal sections of SRA required for resistance. Because the former region contains distinctive features of the amphipathic α-helix involved in VSG dimerization, for example, heptad repeats[7], we introduced point mutations predicted to disrupt this helix. Two independent double mutations (L61P/I62P and I58Q/I62Q) abolished the resistance phenotype, whereas mutations in an adjacent region (V40Q/V43Q/L47Q) did not (Fig. 1, lanes 12–14). Thus, the α-helix at residues 54–65 containing the key hydrophobic residues I58, L61 and I62 was necessary to confer resistance.

The finding that an α-helical region similar to the one involved in the dimerization of VSGs was required for SRA-mediated resistance raised the possibility that SRA neutralizes trypanolytic constituents of NHS through a coiled-coil protein–protein interaction. Therefore, we subjected NHS to affinity chromatography using an N-terminal His-tagged version of SRA (residues 1–251) immobilized onto Ni-nitrilotriacetic acid (NTA) agarose. A 40K doublet was specifically retained by SRA (Fig. 3a, lanes 1, 2), and this occurred in various conditions (pH 7.5 or 5.8 and 0 or 0.6 M NaCl). Notably, the doublet was not observed using L61P/I62P SRA—the α-helix-disrupted mutant SRA that does not confer resistance—whereas the doublet was still present with a functional SRA mutant (Fig. 3a, lanes 3, 4). Similar results were obtained using SRA covalently attached to Sepharose. In this case, the doublet was the only component bound, apart from a 65K contaminant (Fig. 3a, lanes 5, 6). Mass spectrometry identified the 40K doublet as apoL-I, a human apolipoprotein associated with high density lipoprotein (HDL)[8–11] (whereas the 65K protein was serum albumin). Anti-apoL-I antibodies confirmed this finding (Fig. 3a, lanes 7, 8).

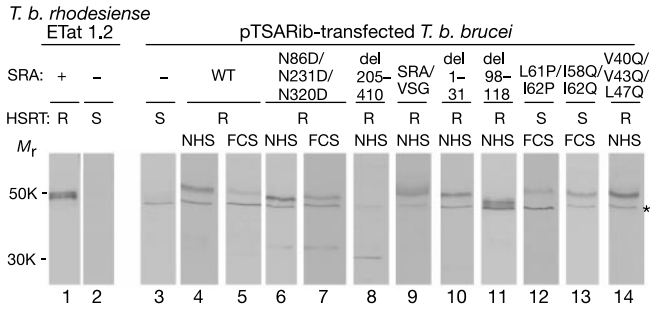

Figure 1 Expression of *SRA* and phenotype of pTSARib-transfected *T. b. brucei*. The western blots obtained with anti-SRA antibodies are shown for *T. b. rhodesiense* ETat 1.2 clones where SRA is expressed (+) or not (−)[4], and for various *T. b. brucei* transformants. The pTSARib vector contained or lacked (−), different versions of *SRA* (WT, wild type; del, deletion of the indicated peptide; SRA/VSG, chimaera of the SRA 1–192 and VSG 288–490 peptides). The cells were analysed by the human serum resistance test (HSRT) *in vivo* and *in vitro*[4], and defined as resistant (R) or sensitive (S). The transformants were grown in mice in the presence of fetal calf serum (FCS) or NHS. The significance of the 45K band (asterisk) is unknown.

The apoL-I gene was amplified by polymerase chain reaction with reverse transcriptase (RT–PCR) from RNA of HepG2 cells and cloned in an expression vector. Various mutants of apoL-I were

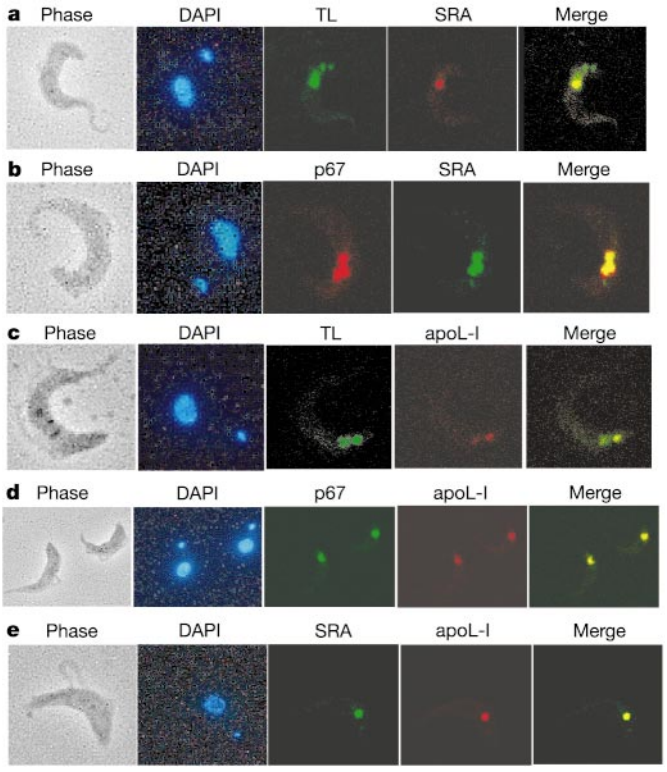

Figure 2 Localization of SRA and apoL-I in the *T. b. rhodesiense* ETat 1.2R clone. The trypanosomes shown in phase contrast were analysed by confocal fluorescence microscopy after incubation for 1 h at 37 °C in the absence (**a**, **b**) or presence (**c**–**e**) of Alexa 594-apoL-I. DAPI (4,6-diamidino-2-phenylindole), tomato lectin (TL) and anti-p67 monoclonal antibodies (p67) label the DNA (large dot, nucleus; small dot, kinetoplast), endocytic compartment and lysosome, respectively[5,6]. Merged images show the localization of SRA or apoL-I with respect to the endocytic compartment and lysosome. Serial sections of these pictures are shown in Supplementary Information.

generated, concentrating on the sequence for a peptide (residues 343–355) exhibiting membrane-disrupting activity *in vitro* (Supplementary Information). In particular, we constructed two truncated versions ending at amino acids 342 and 355, respectively, and a mutant with compromised lipid-destabilizing properties (L345Y/L352A/Y354L)[12]. [^{35}S]-labelled wild-type and mutant versions of apoL-I were synthesized *in vitro* and incubated with His-tagged SRA. [^{35}S]-labelled apoL-I bound to SRA as did the native protein (Fig. 3a, lane 10). No binding occurred using appropriate control resins (no protein or irrelevant His-tagged protein). Notably, [^{35}S]-labelled apoL-I did not bind to one of the helix-disrupted mutants of SRA (L61P/I62P, lane 9), and showed a significantly reduced binding (50%) to the other mutant (I58Q/I62Q). Deletion of the apoL-I C terminus from residue 343 reduced the binding to 5%, whereas the deletion mutant from residue 356 and the L345Y/L352A/Y354L point mutant showed 24% and 67% binding, respectively. These data indicate that the C-terminal region of apoL-I, which contains an amphipathic α-helix[8], is important for the interaction with SRA.

The SRA–apoL-I interaction was confirmed by another approach: incubation with V5-tagged apoL-I led to co-immunoprecipitation of SRA by anti-V5 antibodies (Fig. 3b). In addition, a synthetic peptide corresponding to the α-helix of SRA (amino acids 54–65) appeared to interact directly with the 345–355 peptide of apoL-I, as it abolished the liposome fusogenic activity of apoL-I (Supplementary Information). A model of the interacting helices was built using the known structure of the VSG helices as a basis (Fig. 3c, d). The partners would be in anti-parallel configuration

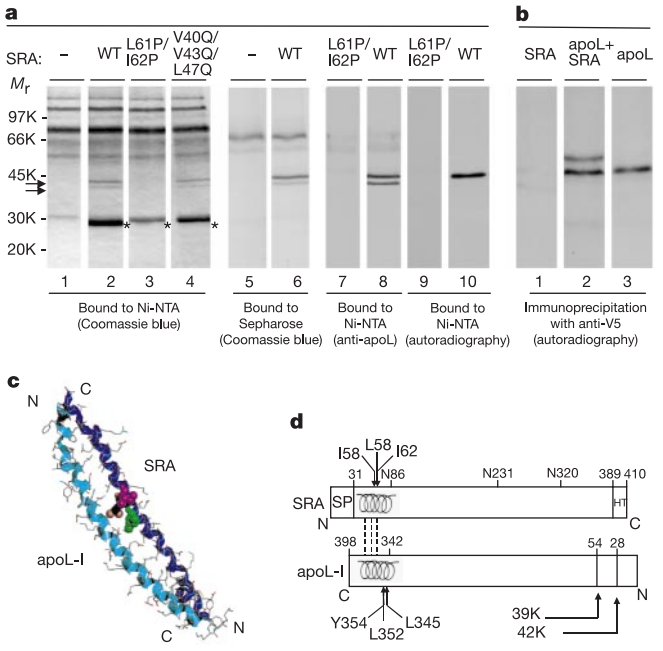

Figure 3 Binding of apoL-I to SRA. **a**, Patterns of NHS proteins bound to resins containing either no protein (–), or different versions of His-tagged SRA. NHS (lanes 1–8) or *in vitro* synthesized [^{35}S]-labelled apoL-I (lanes 9, 10) was incubated with the resin. Bound proteins were eluted with either imidazole (lanes 1–4, 7–10) or deoxycholate (lanes 5, 6), and revealed by Coomassie blue staining (lanes 1–6), binding of anti-apoL-I antibodies (lanes 7, 8) or autoradiography (lanes 9, 10). The double arrow designates bands specifically bound with functional SRA, and asterisks label eluted His-tagged SRA. **b**, Immunoprecipitation with anti-V5 antibodies, of *in vitro* synthesized [^{35}S]-labelled SRA (48K) incubated with or without [^{35}S]-labelled V5–apoL-I (42K). The predicted [^{35}S]-labelled methionine ratio between these proteins is 4:9. **c**, Model of the SRA 31–79 fragment (dark blue ribbon) in anti-parallel interaction with the apoL-I 340–392 fragment (light blue ribbon). I58 (green), L61 (pink) and I62 (mauve) are in CPK representation. **d**, SRA and apoL-I features mentioned in the text (SP, signal peptide; HT, hydrophobic tail; broken lines symbolize the interactions between the α-helices in each molecule).

(−88 and −72 kcal mol^{-1} for the respective hydrophobic energy of the anti-parallel and parallel matchings, to be compared with −89 and −77 kcal mol^{-1} for the interaction between helices A and B in the reference VSG MiTat 1.2 (ref. 7) and in SRA, respectively). The phenotypic effect of the SRA mutants could be explained by differences of complex stability, with −77 and −91 kcal mol^{-1} for the respective hydrophobic energy of the complexes between apoL-I and the I58Q/I62Q and V40Q/V43Q/L47Q SRA mutants, whereas in the L61P/I62P mutant the helical structure is broken and thus no stable complex can be formed.

We investigated the possible involvement of apoL-I in trypanosome lysis. ApoL-I was found to be internalized through the endocytic pathway (Fig. 2c), and to localize with SRA in the lysosome (Fig. 2d, e). Fractionation of NHS on SRA–Sepharose, which essentially retains apoL-I (Fig. 3a, lanes 5, 6), reproducibly

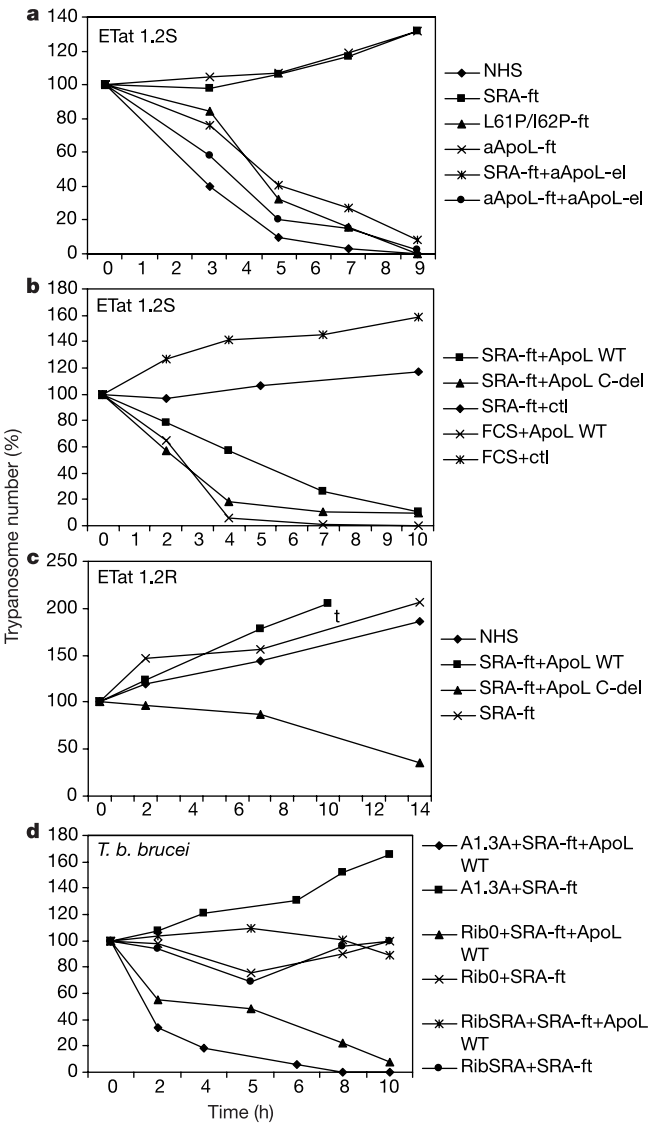

Figure 4 Lytic activity of apoL-I. **a**, Incubation of ETat 1.2S with differently treated NHS (SRA-ft, L61P/I62P-ft, aApoL-ft indicate flow-through fractions from SRA–, L61P/I62P SRA– and anti-apoL-I–Sepharose, respectively; aApoL-el, eluate of the fraction bound to anti-apoL-I–Sepharose). **b**, Incubation of ETat 1.2S in either SRA-ft or FCS supplemented with recombinant apoL-I (C-del, lacking the C-terminal 343–398 peptide) or with the equivalent fraction from control CHO cells (ctl). **c**, Incubation of ETat 1.2R in NHS or SRA-ft supplemented with recombinant apoL-I. **d**, Incubation of different *T. b. brucei* cell lines in SRA-ft supplemented with or without recombinant apoL-I. The pTSARib transformants (Rib0, RibSRA) are pleomorphic forms that do not grow under these incubation conditions.

resulted in total loss of lytic activity, as tested both *in vitro* (Fig. 4a) and in mice (see Methods). This result was not obtained with resins devoid of SRA, or containing L61P/I62P SRA (Fig. 4a). Lytic activity was also lost when NHS was fractionated on anti-apoL-I coupled to Sepharose (Fig. 4a). As expected this resin retained apoL-I, together with various amounts of serum albumin, apolipoprotein J, amyloid protein P and transthyretin (data not shown). Whereas elution of apoL-I from the SRA column required high detergent concentrations, native apoL-I was easily eluted from anti-apoL-I coupled to Sepharose. Addition of this fraction to sera depleted on either SRA– Sepharose or anti-apoL-I–Sepharose completely restored lytic activity (Fig. 4a). To be certain that apoL-I was responsible for this reconstitution, we expressed recombinant His-tagged apoL-I in Chinese hamster ovary (CHO) cells and added the purified protein to NHS that had been depleted using SRA–Sepharose. The addition of physiological concentrations of recombinant apoL-I (around $8\,\mu g\,ml^{-1}$)[8], fully restored the lytic activity on either *T. b. brucei* (AnTat 1.3A and pTSARib-0 transformants) or NHS-sensitive *T. b. rhodesiense* (ETat 1.2S clone), whereas an equivalent extract from control CHO cells did not (Fig. 4b, d). Notably, the same lytic effect of apoL-I was obtained if fetal calf serum was used instead of apoL-I-depleted NHS (Fig. 4b), and lysis was not observed on NHS-resistant cells (either *T. b. rhodesiense* ETat1.2R or *T. b. brucei* pTSARib-SRA) (Fig. 4c, d). Under the same conditions, recombinant apoL-I lacking the 343–398 C-terminal peptide still induced full lysis of NHS-sensitive trypanosomes, but also affected NHS-resistant cells (Fig. 4b, c). Such an effect by an apoL-I mutant deficient in interaction with SRA confirmed that this interaction is involved in resistance to lysis.

Our data show that apoL-I is the trypanolytic factor of NHS and that SRA neutralizes its activity, presumably through a coiled-coil protein–protein interaction. Previous studies identified the lytic factor of NHS as haptoglobin-related protein (Hpr), another HDL-linked serum protein found only in primates[13], but this view was debated[2,14]. Moreover, the suggestion that Hpr might be necessary to allow uptake of the lytic particles into trypanosomes[15], is contradicted by our observation that apoL-I kills trypanosomes in Hpr-free medium. The mechanism of lysis by apoL-I is not understood. Indeed, despite the evidence that lysis by NHS is due to disruption of the lysosomal membrane[1,16], our data show that the fusogenic peptide (residues 343–355) of apoL-I is not required. Resistance to lysis seems to be due to SRA-mediated inhibition of the apoL-I lytic effect within the lysosome. This work opens the way for the characterization of peptides that would be useful for both therapy of sleeping sickness due to *T. b. rhodesiense* and prevention of nagana in cattle. □

Methods

Generation of transgenic trypanosomes expressing SRA mutants

The *SRA* gene in pTSARib-SRA[4] was altered by site-directed mutagenesis (Stratagene) and/or restriction endonuclease digestion and ligation with fragments from the AnTat 11.17 *VSG*[17]. The resultant plasmids were electroporated into *T. b. brucei* procyclic forms that were cyclically transmitted through tsetse flies to obtain bloodstream form transformants[4].

Production of SRA

SRA was produced either by *in vitro* RNA translation using BSDP1400HA65-*SRA*[18], or by expression in *Escherichia coli* using pQE30 in which the 1–753-base-pair *SRA* fragment was inserted between *Bam*HI and *Hin*dIII sites to encode an N-terminal, His-tagged polypeptide. In the latter case, the protein was solubilized from pellets of sonicated cell extracts, by incubation for 1 h at room temperature in 8 M urea, 2 mM mercaptoethanol, 0.1 M NaH_2PO_4, 10 mM Tris (pH 8), then dialysis against the same buffer containing successively 0.5 M urea, 0.35 M urea, 0.1 M urea and 1% CHAPS buffer.

Antibodies

The anti-SRA antibodies were generated by rabbit immunization with the His-tagged 1–251 polypeptide, and affinity purified by binding to antigen-coated nitrocellulose filters and acid elution. They were used after 1:2 and 1:100 dilution, for immunofluorescence and western blot analysis, respectively. The anti-apoL-I antibodies[8] were used at 1:20,000 dilution. Anti-p67 antibodies were from the Ali I-218 hybridoma supernatant (gift of D. G. Russell).

Interaction of SRA with NHS

Recombinant wild type or mutant His-tagged SRA (100 μg) was incubated with 500 μl NHS for 4 h at 4 °C in 0.6 M NaCl, 0.35% CHAPS buffer, 0.15 M MES buffer (pH 5.8) with a cocktail of protease inhibitors (complete EDTA-free including pepstatin, Roche) (buffer A). The mixture was then incubated for 30 min at 4 °C with 100 μl Ni–NTA beads (Qiagen). Processing of these beads, including elution of bound material with 250 mM imidazole, was performed in buffer A as described by Qiagen. Alternatively, His-tagged SRA was covalently coupled to activated CH Sepharose 4B (Pharmacia), and the bound material was eluted in 5% Na deoxycholate, 50 mM Tris (pH 7.5).

Confocal fluorescence microscopy

The trypanosomes were fixed for 10 min in 3.7% paraformaldehyde and permeabilized for 10 min in 0.1% Triton X-100. Biotinylated tomato lectin, Alexa 488-streptavidin and Alexa 488/594-anti-mouse or anti-rabbit secondary antibodies were used. To detect apoL-I, the deoxycholate eluate from SRA–Sepharose was coupled to Alexa 594 after extensive dialysis and depletion of serum albumin by gel filtration, and incubated with trypanosomes for 1 h at 37 °C. The samples were analysed with a Leica TCS SP2 confocal microscope.

Production of native apoL-I

ApoL-I was obtained by elution of the NHS material bound to anti-apoL-I–Sepharose, using 5% CHAPS, 0.1 M glycine (pH 2.8) followed by neutralization with 1 M Tris (pH 8.0). Residual contaminants were identified by mass spectrometry (see text).

Cloning of *apoL-I*

The apoL-I gene was amplified by RT–PCR using total RNA from HepG2 cells and the following pair of oligonucleotides: Apol-F: 5′-TGTCCTCTGCGGTACCATG AGTGCACTTTTCCTTGGTGTGAGAG-3′; Apol-R: 5′-CCCTGCCCTGCTCGAGCAGT TCTTGGTCCGCCTGCAGAATC-3′. The 1.15-kilobase fragment was digested by *Kpn*I and *Xho*I, and ligated with *Kpn*I/*Xho*I-digested pcDNA3.1/V5-HisA plasmid (InVitrogen). Mutants were generated by site-directed mutagenesis (Stratagene) and by deletions and ligations to remove specific fragments.

Interaction of SRA with *in vitro* synthesized apoL-I

[^{35}S]-labelled apoL-I was produced by *in vitro* translation in reticulocyte lysates, using the *apoL-I*-pcDNA3.1/V5-His construct or mutant derivatives as template for transcription. All apoL-I polypeptides contained an in-frame V5 tag at their C terminus, and some were additionally flanked with a C-terminal His tag, depending on the insertion of an in-frame stop codon between the two tag sequences. For interaction with His-tagged SRA, apoL-I with the V5 tag alone was used. In this case, 5 μl reticulocyte lysate containing [^{35}S]-labelled apoL-I was incubated for 4 h at 4 °C with 15 μg His-tagged SRA in buffer A. Further treatment with Ni-NTA beads was performed as described above. The bound/unbound apoL-I was revealed by autoradiography and quantified by liquid scintillation counting after precipitation in 10% trichloroacetic acid.

Modelling

A three-dimensional model of the complex between the apoL-I C-terminal and SRA N-terminal peptides was built using the Swissmodel and Swiss-PDB Viewer programs[19]. The three-dimensional structure of the coiled-coil domain (residues 7–112) of the MiTat 1.2 VSG[7] (Protein data Bank code 2VSG) was used as template. We assumed that the SRA N-terminal and the apoL-I C-terminal fragments interact like the two VSG helices. Residues 31–79 of SRA were aligned to residues 7–54 of the mature VSG (first helix), as that SRA fragment is the most similar to the latter domain of the VSG. ApoL-I residues 340–392 were therefore aligned to residues 59–112 of the VSG (second helix). The parallel (N-C versus N-C) and anti-parallel (N-C versus C-N) matchings were built. The resulting structures were minimized using Hyperchem 5.0 (Hypercube, Inc.), with the conjugate gradient method and AMBER force field. The lowest energy structure was kept. The stereochemical quality of the model was checked with Procheck[20]: 98% of the residues were in the allowed regions of the Ramachandran plot. Molecular views were drawn with the WinMGM program[21].

Dissociation/reconstitution of NHS trypanolytic activity

Untreated, affinity-depleted and/or supplemented serum was added to HMI-9 medium containing 5% CHAPS, to a final concentration of 25%. Recombinant apoL-I was used at physiological concentration ($8\,\mu g\,ml^{-1}$). After a 2 h incubation, CHAPS was removed by extensive dialysis. The trypanosomes were seeded at 5×10^5 cells ml^{-1}. The results shown are representative of at least three separate experiments, and they were confirmed *in vivo*: when directly injected into NMRI mice, the incubation mixtures tested as non-lytic or lytic led to detectable parasitaemia after 2 days or at least 10 days, respectively.

Received 15 November 2002; accepted 3 February 2003; doi:10.1038/nature01461.

1. Hager, K. M. *et al.* Endocytosis of a cytotoxic human high density lipoprotein results in disruption of acidic intracellular vesicles and subsequent killing of African trypanosomes. *J. Cell Biol.* **126,** 155–167 (1994).
2. Raper, J., Portela, M. P., Lugli, E., Frevert, U. & Tomlinson, S. Trypanosome lytic factors: novel mediators of human innate immunity. *Curr. Opin. Microbiol.* **4,** 402–408 (2001).
3. De Greef, C. & Hamers, R. The serum-resistance associated (SRA) gene of *Trypanosoma brucei rhodesiense* encodes a VSG-like protein. *Mol. Biochem. Parasitol.* **68,** 277–284 (1994).
4. Xong, H. V. *et al.* A VSG expression site-associated gene confers resistance to human serum in *Trypanosoma rhodesiense*. *Cell* **95,** 839–846 (1998).
5. Nolan, D. P., Geuskens, M. & Pays, E. N-linked glycans containing linear poly-N-acetyllactosamine as sorting signals in endocytosis in *Trypanosoma brucei*. *Curr. Biol.* **9,** 1169–1172 (1999).
6. Kelley, R. J., Alexander, D. L., Cowan, C., Balber, A. E. & Bangs, J. D. Molecular cloning of p67, a

lysosomal membrane glycoprotein from *Trypanosoma brucei*. *Mol. Biochem. Parasitol.* **98,** 17–28 (1999).
7. Blum, M. L. *et al.* A structural motif in the variant surface glycoproteins of *Trypanosoma brucei*. *Nature* **362,** 603–609 (1993).
8. Duchateau, P. N. *et al.* Apolipoprotein L, a new human high density lipoprotein apolipoprotein expressed by the pancreas. Identification, cloning, characterization, and plasma distribution of apolipoprotein L. *J. Biol. Chem.* **272,** 25576–25582 (1997).
9. Page, N. M., Butlin, D. J., Lomthaisong, K. & Lowry, P. J. The human apolipoprotein L gene cluster: identification, classification, and sites of distribution. *Genomics* **74,** 71–78 (2001).
10. Duchateau, P. N., Pullinger, C. R., Cho, M. H., Eng, C. & Kane, J. P. Apolipoprotein L gene family: tissue-specific expression, splicing, promoter regions; discovery of a new gene. *J. Lipid Res.* **42,** 620–630 (2001).
11. Monajemi, H., Fontijn, R. D., Pannekoek, H. & Horrevoets, A. J. The apolipoprotein L gene cluster has emerged recently in evolution and is expressed in human vascular tissue. *Genomics* **79,** 539–546 (2002).
12. Lins, L., Charloteaux, B., Thomas, A. & Brasseur, R. Computational study of lipid-destabilizing protein fragments: towards a comprehensive view of tilted peptides. *Proteins* **44,** 435–447 (2001).
13. Smith, A. B., Esko, J. D. & Hajduk, S. L. Killing of trypanosomes by the human haptoglobin-related protein. *Science* **268,** 284–286 (1995).
14. Hatada, S. *et al.* No trypanosome lytic activity in the sera of mice producing human haptoglobin-related protein. *Mol. Biochem. Parasitol.* **119,** 291–294 (2002).
15. Drain, J., Bishop, J. R. & Hajduk, S. L. Haptoglobin-related protein mediates trypanosome lytic factor binding to trypanosomes. *J. Biol. Chem.* **276,** 30254–30260 (2001).
16. Shimamura, M., Hager, K. M. & Hajduk, S. L. The lysosomal targeting and intracellular metabolism of trypanosome lytic factor by *Trypanosoma brucei brucei*. *Mol. Biochem. Parasitol.* **115,** 227–237 (2001).
17. Do Thi, C. D., Aerts, D., Steinert, M. & Pays, E. High homology between variant surface glycoprotein gene expression sites of *Trypanosoma brucei* and *Trypanosoma gambiense*. *Mol. Biochem. Parasitol.* **48,** 199–210 (1991).
18. Salmon, D. *et al.* A novel heterodimeric transferrin receptor encoded by a pair of VSG expression site-associated genes in *T. brucei*. *Cell* **78,** 75–86 (1994).
19. Guex, N. & Peitsch, M. C. SWISS-MODEL and the Swiss-PdbViewer: an environment for comparative protein modeling. *Electrophoresis* **18,** 14–23 (1997).
20. Laskowski, R. A., MacArthur, M. W., Moss, D. S. & Thornton, J. M. Procheck: a program to check the stereochemical quality of protein structures. *J. Appl. Crystallogr.* **26,** 283–291 (1993).
21. Brasseur, R. WinMGM: a fast CPK molecular graphics program for analyzing molecular structure. *J. Mol. Graphics* **12,** 212–218 (1994).

Supplementary Information accompanies the paper on *Nature*'s website (**http://www.nature.com/nature**).

Acknowledgements We thank M. Chamekh for the pQ30-SRA plasmid, A. Michel and V. Stroobant for peptide synthesis, S. Kler and C. Flore for technical assistance, and D. Perez-Morza and S. Schurmans for help. This work was supported by the Belgian Fund for Scientific Research (FRSM, FWO and Crédit aux Chercheurs) and by the Interuniversity Attraction Poles Programme, Belgian State, Federal Office for Scientific, Technical and Cultural Affairs. R.B., L.V. and L.L. are, respectively, Research Director and Research Associates at the Belgian Fund for Scientific Research.

Competing interests statement The authors declare that they have no competing financial interests.

Correspondence and requests for materials should be addressed to E.P. (e-mail: epays@ulb.ac.be).

Regulated degradation of a class V myosin receptor directs movement of the yeast vacuole

Fusheng Tang, Emily J. Kauffman, Jennifer L. Novak, Johnathan J. Nau, Natalie L. Catlett* & Lois S. Weisman

Department of Biochemistry, University of Iowa, Iowa City, Iowa 52242, USA

Normal cellular function requires that organelles be positioned in specific locations. The direction in which molecular motors move organelles is based in part on the polarity of microtubules and actin filaments[1–3]. However, this alone does not determine the intracellular destination of organelles. For example, the yeast class V myosin, Myo2p, moves several organelles to distinct locations during the cell cycle[4–8]. Thus the movement of each type of Myo2p cargo must be regulated uniquely. Here we report a regulatory mechanism that specifically provides directionality to vacuole movement. The vacuole-specific Myo2p receptor, Vac17p, has a key function in this process. Vac17p binds simultaneously to Myo2p and to Vac8p, a vacuolar membrane protein. The transport complex, Myo2p–Vac17p–Vac8p, moves the vacuole to the bud, and is then disrupted through the degradation of Vac17p. The vacuole is ultimately deposited near the centre of the bud. Removal of a PEST sequence (a potential signal for rapid protein degradation) within Vac17p causes its stabilization and the subsequent 'backward' movement of vacuoles, which mistargets them to the neck between the mother cell and the bud. Thus the regulated disruption of this transport complex places the vacuole in its proper location. This may be a general mechanism whereby organelles are deposited at their terminal destination.

Genetic studies indicate that Vac8p, a vacuole membrane protein, is required for Myo2p function in vacuole inheritance[9]. However, there was no evidence for a direct interaction between Myo2p and Vac8p. We find here that the protein Vac17p (*Saccharomyces cerevisiae* open reading frame YCL063w), links Myo2p to Vac8p. Vac17p was obtained by several approaches including: (1) identification of the wild-type gene of a newly identified vacuole inheritance mutant *vac17-1* (Fig. 1a); (2) identification of a vacuole-specific, Myo2p-interacting protein[10]; and (3) identification of Vac8p-interacting proteins[11] (and data not shown). We found that the *vac17Δ* mutant was defective in vacuole inheritance (Fig. 1b, c). Thus, Vac17p has an important role in this process.

Several lines of evidence demonstrate that Vac17p functions as the vacuole-specific receptor for Myo2p. First, using immunofluorescence microscopy, Vac17p was found on the vacuole membrane (Fig. 1e). Consistent with this localization, fractionation studies (Fig. 1h) showed that Vac17p was enriched on isolated vacuoles. Second, Vac17p seems to be required only for vacuole inheritance; deletion of *VAC17* did not affect the movement of other Myo2p cargoes[10] and did not show any growth defects (data not shown). Third, Vac17p interacts with Myo2p. Anti-Vac17p antibody precipitated Myo2p (Fig. 1i) and anti-Myo2p antibody precipitated Vac17p (Fig. 1j) from a solubilized crude cell extract. Moreover, Vac17p interacts with Myo2p in a yeast two-hybrid assay[10]. Fourth, the Myo2p–Vac17p interaction is essential for vacuole inheritance. Deletion of the Myo2p-binding region (residues 109–190) of Vac17p blocks vacuole inheritance (Fig. 2c). Furthermore, *myo2* mutants that are specifically defective in vacuole inheritance (*myo2-2*, *myo2-N1304S*) do not interact with Vac17p[10]. Both the defect in vacuole inheritance and the failure of these two *myo2* mutants to interact with Vac17p are suppressed by a point mutation in the Myo2p-binding domain of Vac17p (Vac17p-I140V)[10]. These latter findings indicate that Myo2p and Vac17p directly interact with each other.

We postulated that Vac17p, as the vacuole-specific Myo2p receptor, must attach to the vacuole membrane to function. Vac17p does not appear to contain any transmembrane domains (Fig. 2a). We found that Vac17p–Vac8p interactions are required for normal Vac17p association with the vacuole. In the *vac8Δ* mutant, a significantly smaller portion of Vac17p is associated with the vacuole membrane and much of the Vac17p had an altered location (green dots in Fig. 1f). Moreover, Vac17(Δ319–377)p, which is missing the Vac8p-binding domain, has the same defect in its localization (green dots in Fig. 1g). Similar results were obtained with an *in vitro* analysis of Vac17p distribution. Equal amounts of protein from total cell extracts and isolated vacuoles were separated by SDS–polyacrylamide gel electrophoresis (PAGE) and probed with anti-Vac17p antibody. In the wild-type cells, Vac17p was enriched tenfold in the vacuole fraction. In contrast, in *vac8Δ*, this enrichment was only twofold (Fig. 1h). We noted that both *vac8Δ* and *vac17(Δ319–377)* mutants have greatly elevated levels of

* Present address: Torrey Mesa Research Institute, Syngenta Research and Technology, 3115 Merryfield Row 100, San Diego, California 92121, USA